Pergamon

Tetrahedron 58 (2002) 4237–4244

TETRAHEDRON

Reaction pathways of 2,2,2-trifluoroethylamine and *n*-butylamine with $[Ru(bpy)_2(NO)Cl]^{2+}$

Florencia Di Salvo, Alejandro Crespo, Darío A. Estrin and Fabio Doctorovich*

Departamento de Química Inorgánica, Analítica y Química Física/INQUIMAE, Facultad de Ciencias Exactas y Naturales, Universidad de Buenos Aires, Ciudad Universitaria, Pabellón II, piso 3 (1428), CEHA Buenos Aires, Argentina

Received 12 February 2002; accepted 28 March 2002

Abstract—The reaction of $[Ru(bpy)_2(NO)Cl]^{2+}$ with 2,2,2-trifluoroethylamine produced $[Ru(bpy)_2(NO)Cl]^{+}$ by electron transfer and a number of organic compounds formed via nucleophilic substitution of the intermediate 2,2,2-trifluoroethyldiazonium ion (free or coordinated). Density functional theory computed results suggest that stabilization of the trifluoroethyldiazonium ion by complexation is much larger than the one corresponding to the butyl ion, in agreement with the fact that no rearrangement products derived from $CF_3CH_2^+$ were observed.

1. Introduction

We have recently studied from an experimental and theoretical standpoint the possibility of stabilizing diazonium ions attached to sp^3 carbons by coordination to ruthenium and iron.[1] Experimental results on reaction products as well as density functional theory (DFT) calculations have shown that the butyldiazonium ion might be stabilized by coordination to a $[Ru(bpy)_2Cl]^{+}$ moiety (bpy is 2,2′-bipyridyl). However, direct evidence of the formation of this intermediate could not be found. Although butyldiazonium ion and most of the closely related diazonium ions attached to sp^3 carbons are extremely unstable, a few were observed at low temperature.[2,3] 2,2,2-Trifluoroethyldiazonium ion has been observed by NMR at $-60°C$,[2] and was therefore selected as a good candidate to test the stabilizing effect of $[Ru(bpy)_2Cl]^{+}$. As will be shown below, the electron-attracting effect of the fluorine atoms stabilizes the diazonium ion and increases backdonation from the metal center to the organic moiety. So far there have been a few examples of sp^3 diazonium ions coordinated to molybdenum,[4] tungsten,[5,6] rhenium and cobalt.[7] Our group is exploring the possibility of obtaining stabilized diazonium ions by diazotization of primary amines with coordinated nitrosyl ligands. This would provide an enormous number of possibilities since a large number of amines are easily available.

This route was first pointed out by Meyer et al.,[8] who obtained aromatic diazonium salts stabilized by coordination to ruthenium through the reaction of $[Ru(bpy)_2(NO)Cl]^{2+}$ with aniline and other aromatic amines. Similar reactions involving aliphatic amines could provide insight into the chemistry of the extremely reactive aliphatic diazonium salts if coordination to the metal stabilizes them enough to reduce their reaction rates to a manageable timescale, and if limited amounts of nucleophiles are present. For example, the coordinated diazonium ions could be used as direct sources of free diazonium ions by ligand displacement reactions.

In addition to the experimental study of the reaction pathways of $[Ru(bpy)_2(NO)Cl]^{2+}$ with 2,2,2-trifluoroethylamine, we investigated the structure and stability of the intermediate diazenido by using DFT computations and a continuum solvation model. DFT has proved to be a powerful and economical tool for the investigation of a variety of molecular properties of transition metal compounds.[9,10] Solvation effects can be readily incorporated into the formalism by using continuum[11] and/or discrete solvent models.[12] We have already employed this approach in the investigation of IR spectroscopy, structural properties and reactivity of related Fe and Ru complexes.[3,13–15]

2. Results and discussion

2.1. Formation of products

The products obtained by reaction of $[Ru(bpy)_2(NO)Cl]^{2+}$, **1**, with 2,2,2-trifluoroethylamine, **2**, are shown schematically

Keywords: *n*-butylamine; density functional theory; electron transfer; 2,2,2-trifluoroethylamine; nitrosyl; ruthenium; complex.

* Corresponding author. Tel.: +5411-4576-3358; fax: +5411-4576-3341; e-mail: doctorovich@q1.fcen.uba.ar

0040–4020/02/$ - see front matter
PII: S0040-4020(02)00382-4

in the equation below:

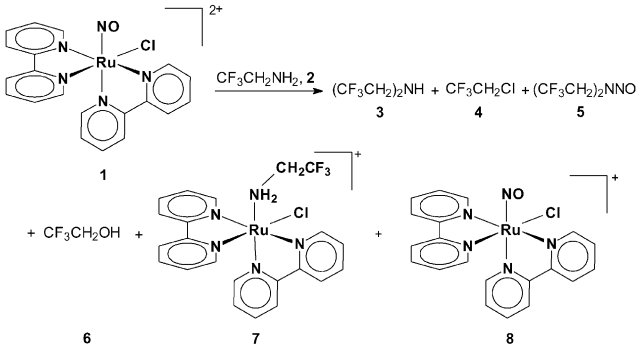

(1)

In the case of **7**, part of the chloride ligand may be replaced by 2,2,2-trifluoroethylamine or CH_3CN. There is also experimental evidence indicating the formation of $[Ru(bpy)_2(NH_2CH_2CF_3)(Cl)]^{2+}$ produced by electron transfer (see below).

As it has been suggested,[1] nucleophilic attack at coordinated NO in **1** by the amine to produce intermediate **9** and subsequent loss of hydroxide to produce the diazenido **10** is proposed (Scheme 1, pathway A). Products **3**, **4** and **6** are formed by nucleophilic attack to the carbocation (or the diazonium salt) by 2,2,2-trifluoroethylamine, chloride ion and hydroxide, respectively (Scheme 1). Although for the sake of simplicity, Scheme 1 shows direct attack on the coordinated diazonium ion, some amount of these products could be produced by attack to the free diazonium ion. Product **5** might be formed by nitrosation of **3** by the nitrosyl complex. It is observed at low amine–complex ratios (1:1 and 2:1). Formation of product **8** might be explained by electron transfer from the amide complex **11** to **1** (Scheme 1, pathway B). DFT calculations show that the electron transfer process is thermodynamically favorable in acetonitrile ($\Delta G^0 = -18.9$ kcal/mol). The amide complex could be produced by trifluoroethylamine proton abstraction from the coordinated amine. The acidity of the coordinated amine is expected to be enhanced due to the electron withdrawing effect of the nearby metal center. It must be noted that the calculations showed that the electron transfer process is thermodynamically unfavorable when the free amine acts as the electron donor.

By observing the FTIR signal at 1931 cm^{-1} (corresponding to the nitrosyl ligand in the starting complex) of reaction mixtures at **1**–**2** ratios varying from 1:1 to 1:15, it could be determined that the stoichiometric ratio is **2**–**1** ≅2.5. The signal corresponding to NO in the starting complex disappeared completely at a **1**–**2** ratio equal to 1:3 while at a 1:2 ratio, it was still observed. This is due to the fact that 1–2 mol of amine are required per mol of complex in order to form the organic products, another mol of **2** is used in the formation of the amine complex **7**, and part of the amine is deactivated by protonation during the reaction. As shown in Table 1, only 25% of organic products are formed with respect to the amount of starting complex when an equimolar ratio of reagents is used. When larger ratios are used, the material balance increases up to 60%, but it stays approximately the same even when a large excess of amine is added. This can be explained taking into account that part of the starting complex is consumed by the electron transfer reaction described above (see the discussion below).

The alcohol (**6**) is practically the only product when the reaction is carried out in the presence of water (CH_3CN–H_2O=4:1). In the presence of a large amount of amine, (*E*)-2,2,2-trifluoroethyldiazoate is observed at short reaction times (3 h) as shown in Table 1 (last column). The large excess of amine makes the reaction medium more basic and favors deprotonation of the diazoic acid **9** (Scheme 1), before loss of OH^- takes place. However, the diazoate decomposes after a few hours, probably by a metal-catalyzed pathway (see below).

2.2. Proposed mechanism

Based on the products obtained in the reaction and in previous results,[3,16] the proposed mechanism for the reaction of trifluoroethylamine with $[Ru(bpy)_2(NO)Cl]^{2+}$, **1**, involves two main pathways (Scheme 1). Pathway A consists of a nucleophilic attack of the amine (**2**) to the nitrosyl ligand to produce a diazoic complex, as previously suggested. The diazoic ligand loses hydroxide to produce the diazenido complex,[17] which may be attacked by different nucleophiles such as the amine itself, chloride or hydroxide to produce **3**, **4** and **6**, respectively. A mechanism involving concerted addition of chloride ion or hydroxide ion through a five- or four-membered transition state cannot be discarded (Eq. (2)). The vacant site might be occupied by **2** or CH_3CN.

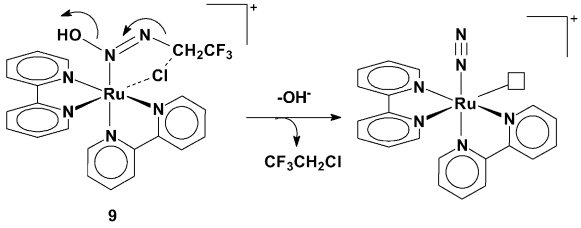

(2)

Regarding the decomposition of product **9**, it must be noted that free (*E*)-trifluoroethanediazoate decomposes slowly even in protic medium[17] and in principle, it is expected to be stable in our reaction medium. A possibility is that the intermediate diazoate decomposes via a metal catalyzed pathway. It is important to note that coordination of trifluoroethanediazoate (or the corresponding diazoic acid) through the nitrogen attached to oxygen should increase rather than decrease the stability of the diazoate due to the expected increase in acidity of the proton attached to the oxygen in the R–N=N(OH) unit.

In the presence of excess amine, the labile N_2 ligand produced by decomposition of the diazonium ion is replaced by trifluoroethylamine to produce the amine complex **7**. Formation of the *N*-nitrosocompound **5** (not shown in Scheme 1) may be explained by nucleophilic attack of the secondary amine **3** to the nitrosyl ligand in **1**.

The other pathway shown in Scheme 1 (pathway B) involves outer sphere electron transfer. Since the hydrogen atoms attached to the amine functionality in **7** are acidic due

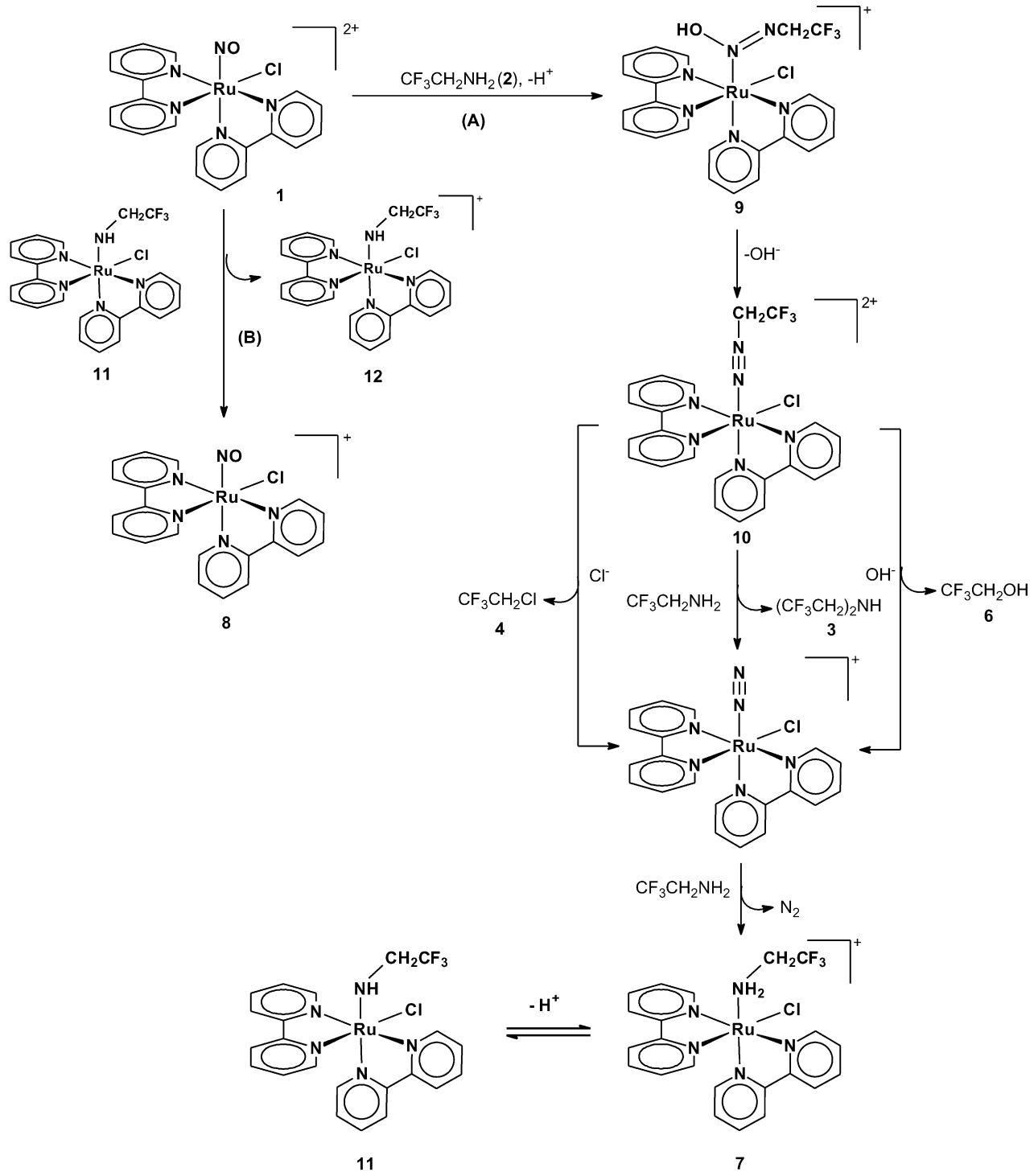

Scheme 1. Proposed mechanism for the reaction of trifluoroethylamine, **2**, with $[Ru(bpy)_2(NO)Cl]^{2+}$, **1**.

Table 1. Organic products obtained by the reaction of $[Ru(bpy)_2(NO)Cl]^{2+}$, **1**, with 2,2,2-trifluoroethylamine, **2**

	1–**2**=1:1	**1**–**2**=1:3	**1**–**2**=1:3	**1**–**2**=1:15
Solvent	CH_3CN	CH_3CN	CH_3CN/H_2O	None
$CF_3CH_2NHCH_2CF_3$ (**3**)	5	ca. 10[a]	ca. 10[a]	14
CF_3CH_2Cl (**4**)	7	19	<1	17
$CF_3CH_2N(NO)CH_2CF_3$ (**5**)	2	<1	4	2
CF_3CH_2OH (**6**)	11	30	25	16
$CF_3CH_2NNO^-$	<1	<1	<1	16

Results were obtained by ^1H NMR as described in Section 8. They are expressed as moles of product per 100 mol of starting complex.
[a] The ^1H NMR quartet corresponding to this product overlapped with the quartet corresponding to **2**.

Table 2. Organic products obtained by the reaction of $[Ru(bpy)_2(NO)Cl]^{2+}$, **1**, with *n*-butylamine (**1**–$BuNH_2$=1:3)

	Yield (%)
1-Butene	8.5
trans-2-Butene	4.9
cis-2-Butene	4.0
1-Chlorobutane	5.6
2-Chlorobutane	1.9
1-Butanol	7.2
2-Butanol	<1
Dibutylamine	6.5
N-Butyl-1-butanimine	2.0
Butyronitrile	21

Results are expressed as moles of product per 100 mol of starting complex.

to the proximity of the electron attracting metal center, a certain amount of coordinated amide complex **11** can be in equilibrium with the corresponding amine complex **7**. Electron transfer from the amide complex to **1** produces the reduced NO complex **8**. It has been established that **8** is produced by electrochemical reduction of **1**,[18] although to our knowledge it is the first time that one-electron reduction of $[Ru(bpy)_2(NO)Cl]^{2+}$ is observed in this kind of reaction (namely, addition of amines to NO complexes).

The determined yield for **8** was found to be 36% in a 1:3 reaction mixture. This result indicates that under these conditions 36% of the starting complex reacted by electron transfer and 64% reacted by the nucleophilic route, which gives raise to the organic products. This is in good agreement (considering the experimental errors) with the 59% material balance for the organic products shown in Table 1 for the 1:3 reaction (second column). At this point, we would like to make clear that we believe that the equilibrium among **11** and **7** is presumably displaced to the right under the reaction conditions; a small amount of **11** present in steady state concentration is enough to react via the electron transfer pathway. The yield of **7** would be therefore indicative of how much of **11** (or **7**) reacted by the electron transfer pathway. The isolated yield for **7** was determined to be 26% in a 1:3 reaction, therefore it can be deduced that approximately 64−26=38% (the amount of **7** produced by the nucleophilic route minus its isolated amount) of **11** reacted by electron transfer, which is in good agreement with the 36% yield obtained for **8** and is consistent with the proposed mechanism.

An interesting point to discuss is related to the large difference in reactivity exhibited by trifluoroethylamine as compared to *n*-butylamine. In a previous work[1] we have studied the reaction of *n*-butylamine with the same complex obtaining a large amount of rearrangement products derived from the free carbocation (Bu^+) such as alkenes, 2-butanol and 2-chlorobutane, as seen in Table 2. In the case of the trifluoroethyldiazonium ion, although the main decomposition product is expected to be trifluorodiazoethane (by rapid proton loss),[17] we found no evidence for its formation. We believe that the complete absence of this product or other rearrangement products in the case of trifluoroethylamine is mainly due to two factors, being the larger stability and electrophilicity of the intermediate diazonium ion derived from trifluoroethylamine as compared to the one derived from *n*-butylamine, in agreement with the computational results (see below). Both factors would tend to favor the reaction of the postulated diazonium ion with hydroxide ion or chloride ion before decomposition takes place.

As it can be observed in Table 2, the total amount of organic products for the *n*-butylamine reaction is around 65% (practically the same as in the 2,2,2-trifluoroethylamine case). This fact plus the observation of an FTIR signal at 1640 cm^{-1} in the reaction mixture (attributable to the reduced complex **8**) indicates that part of the initial complex **1** is consumed by the electron transfer reaction shown in Scheme 1 (pathway B) also in the case of *n*-butylamine.

2.3. Computed coordination geometries

The optimized structures of $[Ru(bpy)_2Cl(N_2R)]^{2+}$ (R=butyl, phenyl or trifluoroethyl) are shown in Fig. 1. Relevant geometrical parameters are presented in Table 3.

Regarding the reliability of our DFT scheme in predicting

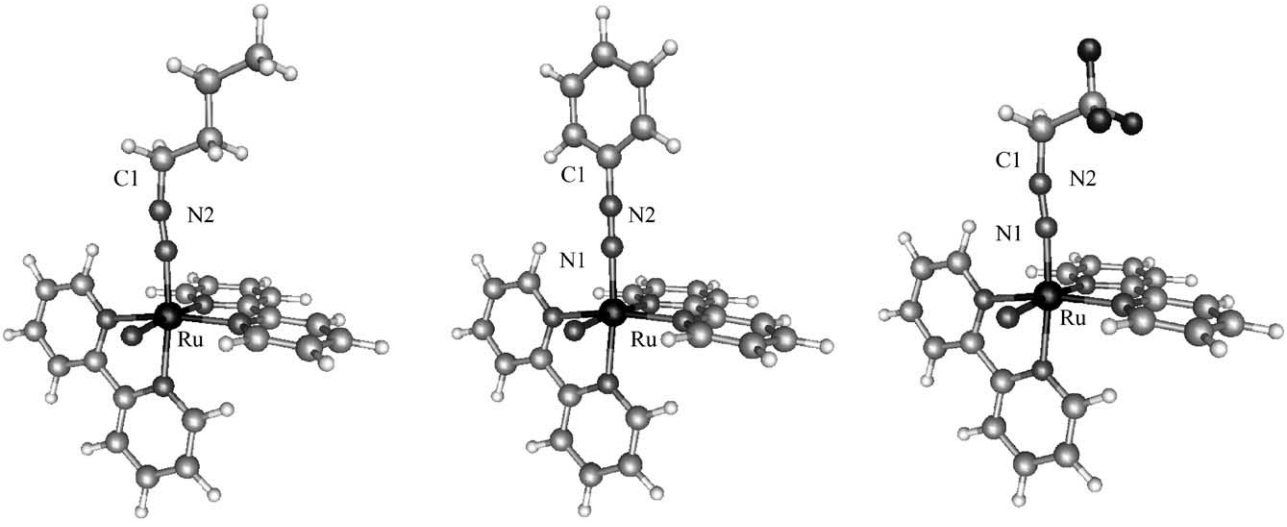

Figure 1. Structure of $[Ru(bpy)_2(Cl)R]^{2+}$, (R=BuN_2, PhN_2, $CF_3CH_2N_2$).

Table 3. Selected optimized bond distances and angles (Å and degrees)

	C1–N2	N1–N2	Ru–N1	N–O	Ru–N1–N2	N1–N2–C1
N_2	–	1.112	–		–	–
$[CF_3CH_2N_2]^+$	1.402	1.112	–		–	177.7
$[BuN_2]^+$	1.415	1.113	–		–	176.0
$[PhN_2]^+$	1.358	1.111	–		–	179.9
$[Ru(bpy)_2(Cl)N_2]^{2+}$	–	1.117	1.942		178.3	–
$[Ru(bpy)_2(Cl)N_2CH_2CF_3]^{2+}$	1.402	1.150	1.821		173.8	169.3
$[Ru(bpy)_2(Cl)N_2Bu]^{2+}$	1.410	1.142	1.849		173.5	167.8
$[Ru(bpy)_2(Cl)N_2Ph]^{2+}$	1.360	1.152	1.855		178.7	176.9
$[Ru(bpy)_2(Cl)NO]^{2+}$			1.775	1.142		
$[Ru(bpy)_2(Cl)NO]^{+}$			1.841	1.183		
$[Ru(bpy)_2(Cl)NO]^{2+}$ Exp.[a]			1.749	1.131		

[a] Ref. 31.

the geometries of Ru complexes, previous results for $[Ru(NH_3)_5Pz]^{2+}$ compared very well with experiment.[14] A comparison of our computed geometry for $[Ru(bpy)_2ClN_2]^+$ with experimental results[19] for $[Ru(bpy)_2Cl_2](H_2O)_5$ and $[Ru(bpy)_2Cl(CO)][ClO_4]$ has been made in order to gauge the quality of our results in bipyridil complexes. The computed Ru–Cl bond distance is 2.440 Å, compared with the experimental results of 2.427 and 2.392 Å for $[Ru(bpy)_2Cl_2](H_2O)_5$ and $[Ru(bpy)_2Cl(CO)][ClO_4]$, respectively. The Ru–N distances range from 2.012 to 2.051 Å in our computed geometry and from 2.013 to 2.052 and 2.068 to 2.178 Å in the $[Ru(bpy)_2Cl_2](H_2O)_5$ and $[Ru(bpy)_2Cl(CO)][ClO_4]$, respectively. Regarding bond angles, the N–Ru–N angle within the heterocyclic ring is 79.2° in $[Ru(bpy)_2Cl_2](H_2O)_5$, ranges from 76.8 to 78.7° in $[Ru(bpy)_2Cl(CO)][ClO_4]$, and from 78.3 to 79.6° in our optimized $[Ru(bpy)_2ClN_2]^+$ structure. It can be noted that the computed geometrical parameters compare very well with experimental data.

The computed structures of the complexes show that the aryl species is practically linear, while in the aliphatic complexes there are larger deviations from linearity, with Ru–N1–N2 and C1–N2–N1 angles of 173.8 and 169.3°, respectively, for the trifluoroethyldiazenido complex. N1–N2 bond distances in the free diazonium salts and the coordinated N_2 complex are smaller than in the diazenido derivatives, reflecting in the last case less triple bond character as a consequence of back-donation. Interestingly, the larger degree of back-donation in the diazenido complexes compared to the N_2 coordinated system is also reflected in the Ru–N1 bonds, which are considerably shorter in the diazenido species, consistently with a stronger Ru–N bond. As expected for the strong electron attracting character of the fluoride substituents, the shortest Ru–N1 bond corresponds to trifluoroethyldiazenido.

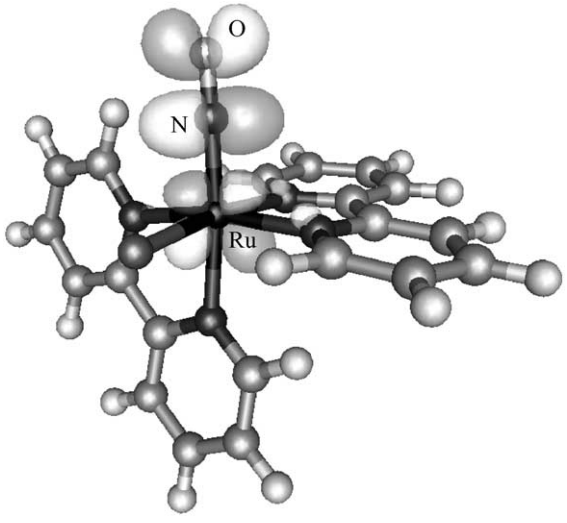

Figure 2. LUMO of $[Ru(bpy)_2Cl(NO)]^{2+}$.

We have also performed geometry optimizations of the reactant $[Ru(bpy)_2Cl(NO)]^{2+}$, **1**, and of the reduced species $[Ru(bpy)_2Cl(NO)]^+$, **8**. For the reactant, the computed results agree very well with experiment.[20] It can be noted that there is an increase in the NO bond distance upon reduction. This can be explained by considering that the LUMO of **1** (Fig. 2) has a significant contribution of the π^* NO orbital. It can also be noted that the Ru–N bond distance of the reduced species is substantially larger than the one corresponding to the reactant.

2.4. Stabilization by complexation: computational results

Table 4 shows ΔE values for the decomposition reaction of $[Ru(bpy)_2(N_2R)]^{2+}$ (Eq. (3), R=Ph, Bu, CF_3CH_2) and the free diazonium ions. It can be observed in the table that stabilization of the trifluoroethyldiazenido ligand due to complexation (B3LYP-PCM) is closer to the highly stable benzenediazenido than to the butyldiazenido. The large stabilization of the trifluoroethyldiazenido is mainly due to instability of the carbocation, induced by the electron-attracting fluoride substituents.

$$[Ru(bpy)_2(N_2CF_3CH_2)Cl]^{2+} \rightarrow [Ru(bpy)_2(N_2)Cl]^+ + CF_3CH_2^{\oplus} \quad (3)$$

In vacuo, the order of stability for the free diazonium ions is Ph>trifluoroethyl>butyl, as expected. It is interesting to remark that in vacuo, complexation leads to an important decrease of the computed C–N bond dissociation energies. This is probably explained by the fact that complexation brings together two positive species. On the other hand, in acetonitrile solution, our computations predict an important stabilization of the diazenido ligands by complexation. The effect of the solvent may be understood in terms of a charge

Table 4. C–N bond dissociation energies (kcal/mol)

	B3LYP	B3LYP-PCM
$[CF_3CH_2N_2]^+$	22.2	26.6
$[Ru(bpy)_2(Cl)N_2CH_2CF_3]^{2+}$	6.5	34.6
$[BuN_2]^+$	8.1	10.2
$[Ru(bpy)_2(Cl)N_2Bu]^{2+}$	−17.9	25.6
$[PhN_2]^+$	37.4	37.1
$[Ru(bpy)_2(Cl)N_2Ph]^{2+}$	11.8	40.9

stabilization effect: the dielectric stabilizes more effectively the doubly charged diazenido complex than the singly charged products. On the other hand, solvation does not significantly affect the computed results for the free diazonium ions.

Strengthening of the N–C bond in a diazenido ligand by complexation is not the only important feature to be considered in order to predict its stability. The electrophilicity of the carbon atom attached to nitrogen has to be taken into account since nucleophilic attack to this carbon will also break the N–C bond. As it can be seen in Table 5, all considered diazonium ions are thermodynamically unstable towards nucleophilic attack of hydroxide ion or the corresponding amine. We can relate the computed ΔE values with the relative stabilities of the diazonium ions in solution by assuming that the activation energies, and therefore the reaction rates correlate with the thermodynamical ΔE values.

It can be seen in Table 5 that the reaction of the trifluoroethyldiazenido ligand with hydroxide is thermodynamically more favorable than that of butyldiazenido and benzenediazenido due to the electron-attracting effect of the fluoride substituents and correlates with the stabilities of the corresponding carbocations. Assuming that the reaction rates correlate with the thermodynamical ΔE values, we could say that the trifluoroethyldiazenido is more nucleophilic than the butyldiazenido and benzenediazenido. However, in our experimental situation, the diazenido could also be attacked by the corresponding amine to produce a secondary amine plus a nitrogen complex, as it has been observed before.[16] Table 5 shows that in this situation, the trifluoroethyldiazenido ligand is less prone to attack than the butyldiazenido ligand. In conclusion, on one hand, there is an important strengthening of the N–C bond that makes the trifluoroethyldiazenido ligand more stable than its butyl analog, but on the other hand, the increased electrophilicity of the trifluoroethyldiazenido makes the reaction toward hydroxide more favorable than in the case of the butyldiazenido. This is consistent with the results shown in Tables 1 and 2: the yield for the corresponding alcohol is 30% for the 2,2,2-trifluoroethylamine reaction, while only 7% of alcohol is obtained in the reaction of *n*-butylamine under the same conditions.

3. Computational methodology

The calculations were performed using a Gaussian basis set implementation of DFT.[21] The Kohn–Sham self-consistent procedure was applied for obtaining the electronic density and energy through the determination of a set of one-electron orbitals.[22] Gaussian basis sets were used for the expansion of the one-electron orbitals and also for the additional auxiliary set used for expanding the electronic density. Matrix elements of the exchange-correlation potential were calculated by a numerical integration scheme.[23] The orbital and auxiliary basis sets optimized by Sim et al.[24] for DFT calculations were used for C, N, and H atoms. Basis sets for Ru were taken from Ref. 25. The contraction patterns were (5211/411/1) for C, and N (633321/53211/531) for Ru, and (41/1) for H. The contraction patterns for the electronic density expansion sets are: (1111111/111/1) for C and N, (1111111111/11111/11111) for Ru, and (111111/1) for H. A more detailed description of the technical aspects of the program is given in Ref. 21.

Geometries were optimized for the isolated systems within the local density approximation (LDA) using the Vosko–Wilk–Nusair correlation functional.[26] It has been shown that LDA performs well in predicting bond distances and angles in Werner-type transition metal complexes.[27] Single point calculations were performed at the LDA gas phase optimized geometries using the hybrid B3LYP exchange-correlation functional.[28]

Solvent effects were modeled using the polarized continuum model (PCM) scheme. The PCM implementation given in Ref. 29, in which the self-consistency between the solute wavefunction and solvent polarization is achieved during the self-consistent field cycle, has been employed. PCM computations have been performed using the GAUSSIAN 98 software package.[30]

4. Experimental

4.1. General comments

Unless otherwise noted, all manipulations were performed with exclusion of oxygen and moisture using standard Schlenk procedures. ^1H, ^{13}C and ^{15}N NMR spectra were recorded using a Bruker AM500 equipped with a broadband probe. ^1H, ^{13}C and ^{15}N NMR shifts are reported relative to CD_3CN (δ=1.95, 1.80 and −136 ppm, respectively). IR

Table 5. Energetic changes (kcal/mol) for nucleophilic substitution in diazonium salts

Reaction	B3LYP	B3LYP-PCM
$OH^- + CF_3CH_2N_2^+ \rightarrow N_2 + CF_3CH_2OH$	−247.1	−105.7
$OH^- + BuN_2^+ \rightarrow N_2 + BuOH$	−221.6	−86.8
$OH^- + PhN_2^+ \rightarrow N_2 + PhOH$	−223.3	−95.7
$CF_3CH_2NH_2 + CF_3CH_2N_2^+ \rightarrow N_2 + (CF_3CH_2)_2NH_2^+$	−65.6	−60.0
$BuNH_2 + BuN_2^+ \rightarrow N_2 + (Bu)_2NH_2^+$	−70.1	−63.3
$PhNH_{2+}PhN_2^+ \rightarrow N_2 + (Ph)_2NH_2^+$	−53.3	−49.0

spectra were recorded using a Nicolet 510P FTIR spectrometer with a Spectra Tech cell for liquids with CaF_2 windows. UV–visible spectra were recorded using a Hewlett-Packard 8453 spectrometer. Gas chromatograms were done on a Shimadzu GC-17A gas chromatograph. GC–mass spectra were recorded on a Shimadzu GC-17A gas chromatograph attached to a GCMS-QP5000S mass spectrometer. In both chromatographs, a tandem consisting of two capillary Supelco SPB5 and SE54 columns was used (60 m×0.32 mm each). Chemical analyses were performed with a Carlo Erba EA 1108 microanalyzer.

4.2. Reagents

Acetonitrile and methanol were purchased from J. T. Baker and distilled from CaH_2· CD_3OD, CD_3CN, $[RuCl_2(bpy)_2]$ and 2,2,2-trifluoroethylamine were purchased from Aldrich and used as received. $Na^{15}NO_2$ was purchased from MSD Isotopes. $[Ru(bpy)_2Cl(NO)](PF_6)$[18] and $[Ru(bpy)_2Cl(NO_2)]$[31] were prepared by known procedures. $[Ru(bpy)_2Cl(NO)](PF_6)_2$ was prepared from $RuCl_2(bpy)_2$ by modifying a previously reported procedure:[31] the synthesis was carried out under an inert atmosphere of nitrogen. The $[Ru(bpy)_2Cl(NO)](PF_6)_2$ complex so obtained was orange, instead of brown or green as obtained by the original technique. The difference was probably due to contamination of the green sample with a small amount of oxo complex. Anal. calcd: C, 31.24; N, 9.11; H, 2.10; found: C, 31.20; N, 9.38; H, 2.08. $[Ru(bpy)_2Cl(^{15}NO)](PF_6)_2$ was prepared by this same procedure, using $Na^{15}NO_2$ instead of $NaNO_2$.

4.3. Reactions of 2,2,2-trifluoroethylamine with $[Ru(bpy)_2Cl(NO)](PF_6)_2$

In all cases, the mixtures were transferred to the corresponding vessel after the reaction was completed with the aid of syringes and under inert atmosphere. The reaction mixtures were analyzed by UV–visible, FTIR and NMR spectroscopies. When NMR spectra were ran on the reaction mixtures, CD_3CN was used as the reaction solvent instead of CH_3CN. In the cases that UV–visible spectra were determined, the reaction mixture was diluted around 2000 times with CH_3CN.

4.4. Reactions in solution

2,2,2-Trifluoroethylamine (3.2 μL, 0.04 mmol for the 1:1 reaction; 9.6 μL, 0.12 mmol for the 3:1 reaction) was added to a solution of 30.4 mg (0.04 mmol) of $[Ru(bpy)_2Cl(NO)](PF_6)_2$ in 0.5 mL of acetonitrile in a 5 mL round-bottomed flask. After a few minutes, the original orange solution changed to dark red. It was allowed to react at room temperature for 2 days protected from light.

4.5. Heterogeneous reaction

2,2,2-Trifluoroethylamine (48 μL, 0.6 mmol) was added to 30.4 mg (0.04 mmol) of $[Ru(bpy)_2Cl(NO)](PF_6)_2$. The solid was totally dissolved by the amine producing a dark red solution. The reaction mixture was allowed to react for 3 h at room temperature protected from light.

4.5.1. Product identification and isolation. Compounds **3**, **4**, **6** and (*E*)-2,2,2-trifluoroethyldiazoate were identified by comparison of their spectroscopical properties with authentic samples. Yields were determined by comparing the integrations due to the ^1H NMR signals corresponding to the bipyridine ligand (which was used as an internal standard) with those corresponding to the products.

*Data for $CF_3CH_2NHCH_2CF_3$ (**3**).* ^1H NMR (CD_3CN): δ=3.7 ppm (q), J_{HF}=6.6 Hz. ^{13}C NMR (CD_3CN): δ = 45.7 ppm (q).[32]

*Data for CF_3CH_2Cl (**4**).* ^1H NMR (CD_3CN): δ=4.1 ppm (q), J_{HF}=8.5 Hz. ^{13}C NMR (CD_3CN): δ=43.5 ppm (q).[32] GC–MS (70 eV); *m/z* (relative intensity): 120 (24, M^+), 118 (71), 83 (42), 69 (12).

*Data for $CF_3CH_2N(NO)CH_2CF_3$ (**5**).* ^1H NMR (CD_3CN): δ=5.1 ppm (q), J_{HF}=4.4 Hz. ^{15}N NMR (CD_3CN): δ=192 ppm (corresponding to $CF_3CH_2N^{15}NO$). FTIR (CH_3CN): ν(NNO)=1631.8 cm^{-1}; $\nu(N^{15}NO)$=1590 cm^{-1}.

*Data for CF_3CH_2OH (**6**).* ^1H NMR (CD_3CN): δ=3.9 ppm (q), J_{HF}=9.1 Hz. ^{13}C NMR (CD_3CN): δ=60.0 ppm (q).[32]

Data for (E)-2,2,2-trifluoroethyldiazoate ($CF_3CH_2N{=}NO^-$). ^1H NMR (CD_3CN): δ=4.0 ppm (q), J_{HF}=10.6 Hz.[17]

$[Ru(bpy)_2NH_2CH_2CF_3(X)]$ where X=Cl^- (compound **7**) or CH_3CN, was obtained by precipitation from the reaction mixture at −18°C and isolated by centrifugation. Then the dark orange solid was identified by ^1H NMR (CD_3CN): δ=3.77 ppm (broad), ^{13}C NMR (CD_3CN): δ=41.9 ppm (q).[32] *m/z*: 443 ($[Ru(bpy)_2NH_2CH_2CF_3]$–CF_3). Isolated yield: 26%.

Compound **8** ($[Ru(bpy)_2(Cl)NO]^+$) was isolated from the reaction mixture by column chromatography with silica gel. CH_3OH–HCl=100:1 was used as the solvent system. Compound **8** was identified by comparison of its UV–visible and FTIR spectra with those previously reported.[18] Although we could not get a good isolated yield for **8** due to its instability (it oxidizes rather easily), we determined its yield to be 36% by looking at its corresponding UV–visible band at 310 nm in a 1:3 reaction mixture (ε=1.62×10^4).[18]

A broad signal attributable to a Ru(III) amine complex was observed by ^{13}C NMR of the reaction mixture. ^{13}C NMR (CD_3CN): δ=43.5 ppm.[32]

Acknowledgements

This work was supported by University of Buenos Aires (project TX-042), VW Stiftung and ANPCYT (project # 06-00000-01704). We thank the Cambridge Crystallographic Data Center for having provided us the Cambridge Structural Database Version 5.18. F. D. and D. A. E. are members of the scientific staff of CONICET. F. D. S. and A. C. are UBA fellows.

References

1. Doctorovich, F.; Escola, N.; Trápani, C.; Estrin, D. A.; Turjanski, A. G.; González Lebrero, M. C. *Organometallics* **2000**, *19*, 3810.
2. Mohrig, J. R.; Keegstra, K. *J. Am. Chem. Soc.* **1967**, *89*, 5492.
3. Berner, D.; McGarrity, J. F. *J. Am. Chem. Soc.* **1979**, *101*, 3135.
4. Herrmann, W. A.; Biersack, H. *Chem. Ber.* **1977**, *110*, 896.
5. Diamantis, A. A.; Chatt, J.; Leigh, J. G.; Heath, G. A. *J. Organomet. Chem.* **1975**, *84*, C11.
6. Hillhouse, G. L.; Haymore, B. L.; Herrmann, W. A. *Inorg. Chem.* **1979**, *18*, 2423.
7. Casey, C. P.; Widenhoefer, R. A.; Hayashi, R. K. *Inorg. Chem.* **1995**, *34*, 2258.
8. Bowden, W. L.; Little, W. F.; Meyer, T. J. *J. Am. Chem. Soc.* **1977**, *99*, 4340.
9. Li, J.; Noodleman, L.; Case, D. A. Electronic Structure Calculations: Density Functional Methods with Applications to Transition Metal Complexes. In *Inorganic Structure and Spectroscopy*; Solomon, E. I., Lever, B. P., Eds.; Wiley: New York, 1999.
10. Deeth, R. J. *Computational Modeling of Transition Metal Centers*; *Structure and Bonding*, Vol. 82; Springer: Berlin, 1995.
11. Cramer, C. J.; Truhlar, D. G. In *Quantitative Treatments of Solute/Solvent Interactions*; Politzer, P., Murray, J. S., Eds.; Elsevier: New York, 1994.
12. Ho, L. L.; MacKerell, A. D.; Bash, P. A. *J. Phys. Chem.* **1996**, *100*, 4466.
13. Estrin, D. A.; Baraldo, L. M.; Slep, L. D.; Barja, B. C.; Olabe, J. A. *Inorg. Chem.* **1996**, *35*, 3897.
14. Hamra, O. Y.; Slep, L. D.; Olabe, J. A.; Estrin, D. A. *Inorg. Chem.* **1998**, *37*, 2033.
15. Estrin, D. A.; Hamra, O. Y.; Paglieri, L.; Slep, L. D.; Olabe, J. A. *Inorg. Chem.* **1996**, *35*, 6832.
16. Doctorovich, F.; Trápani, C. *Tetrahedron Lett.* **1999**, *40*, 4635.
17. Ho, J.; Fishbein, J. C. *J. Am. Chem. Soc.* **1994**, *116*, 6611.
18. Callahan, R. W.; Meyer, T. J. *Inorg. Chem.* **1977**, *3*, 16.
19. (a) Eggleston, D. S.; Goldsby, K. A.; Hodgson, D. J.; Meyer, T. J. *Inorg. Chem.* **1985**, *24*, 4573. (b) Clear, J. M.; Kelly, J. M.; O'Connel, C. M.; Vos, J. G.; Cardin, C. J.; Costa, S. R.; Edwards, A. J. *J. Chem. Soc., Chem. Commun.* **1980**, 750.
20. Nagao, H.; Nishimura, H.; Funato, H.; Ichikawa, Y.; Howell, F. S.; Mukaida, M.; Kakihana, H. *Inorg. Chem.* **1989**, *28*, 3955.
21. Estrin, D. A.; Corongiu, G.; Clementi, E. In *METECC, Methods and Techniques in Computational Chemistry*; Clementi, E., Ed.; Stef: Cagliari, 1993; Chapter 12.
22. Kohn, W.; Sham, L. *J. Phys. Rev.* **1965**, *A140*, 1133.
23. Becke, A. D. *J. Chem. Phys.* **1988**, *88*, 1053.
24. (a) Sim, F.; Salahub, D. R.; Chin, S.; Dupuis, M. *J. Chem. Phys.* **1991**, *95*, 4317. (b) Sim, F.; St-Amant, A.; Papai, Y.; Salahub, D. R. *J. Am. Chem. Soc.* **1992**, *114*, 4391.
25. Godbout, N.; Salahub, D. R.; Andzelm, J.; Wimmer, E. *Can. J. Chem.* **1992**, *70*, 560.
26. Vosko, S. H.; Wilk, L.; Nusair, M. *Can. J. Chem.* **1980**, *58*, 1200.
27. (a) Bray, M. R.; Deeth, R. J.; Paget, V. J.; Sheen, P. D. *Int. J. Quantum Chem.* **1996**, *61*, 85. (b) Sosa, C.; Andzelm, J.; Elkin, B. C.; Wimmer, E. *J. Phys. Chem.* **1992**, *96*, 6630.
28. (a) Becke, A. D. *J. Chem. Phys.* **1993**, *98*, 5648. (b) Lee, C.; Yang, W.; Parr, R. G. *Phys. Rev. B* **1988**, *37*, 785.
29. Cossi, M.; Barone, V.; Cammi, R.; Tomasi *J. Chem. Phys. Lett.* **1996**, *255*, 327.
30. Frisch, M. J.; Trucks, G. W.; Schlegel, H. B.; Scuseria, G. E.; Robb, M. A.; Cheeseman, J. R.; Zakrzewski, V. G.; Montgomery, Jr., J. A.; Stratmann, R.; Burant, J.; Dapprich, S.; Millam, J. M.; Daniels, A. D.; Kudin, K. N.; Strain, M. C.; Farkas, O.; Tomasi, J.; Barone, V.; Cossi, M.; Cammi, R.; Mennucci, B.; Pomelli, C.; Adamo, C.; Clifford, S.; Ochterski, J.; Petersson, G. A.; Ayala, P. Y.; Cui, Q.; Morokuma, K.; Malick, D. K.; Rabuck, A. D.; Raghavachari, K.; Foresman, J. B.; Cioslowski, J.; Ortiz, J. V.; Baboul, A. G.; Stefanov, B. B.; Liu, G.; Liashenko, A.; Piskorz, P.; Komaromi, I.; Gomperts, R.; Martin, R. L.; Fox, D. J.; Keith, T.; Al-Laham, M. A.; Peng, C. Y.; Nanayakkara, A.; Gonzalez, C.; Challacombe, M.; Gill, P. M. W.; Johnson, B.; Chen, W.; Wong, M. W.; Andres, J. L.; Gonzalez, C.; Head-Gordon, M.; Replogle, E. S.; Pople, J. A. *Gaussian 98*, Rev. A7, Gaussian, Inc.: Pittsburgh, PA, 1998.
31. Godwin, J. B.; Meyer, T. J. *Inorg. Chem.* **1971**, *10*, 471.
32. The ^{13}C NMR signal corresponding to the CF_3 unit was not observed due to the C–F splitting.